Chinese Journal of Natural Medicines

An inulin-type fructan CP-A from *Codonopsis pilosula* attenuates experimental colitis in mice by promoting autophagy-mediated inactivation of NLRP3 inflammasome

Jiangtao ZHOU, Jun WANG, Jiajing WANG, Deyun LI, Jing HOU, Jiankuan LI, Yun'e BAI, Jianping GAO

Citation: Jiangtao ZHOU, Jun WANG, Jiajing WANG, Deyun LI, Jing HOU, Jiankuan LI, Yun'e BAI, Jianping GAO, An inulin-type fructan CP-A from *Codonopsis pilosula* attenuates experimental colitis in mice by promoting autophagy-mediated inactivation of NLRP3 inflammasome, Chinese Journal of Natural Medicines, 2024, 22(3), 249-264. doi: 10.1016/S1875-5364(24)60556-X.

View online: https://doi.org/10.1016/S1875-5364(24)60556-X

Available online at www.sciencedirect.com
ScienceDirect
Chinese Journal of Natural Medicines 2024, **22**(3): 249-264
doi: 10.1016/S1875-5364(24)60556-X
Chinese Journal of Natural Medicines

•Original article•

An inulin-type fructan CP-A from *Codonopsis pilosula* attenuates experimental colitis in mice by promoting autophagy-mediated inactivation of NLRP3 inflammasome

ZHOU Jiangtao[Δ], WANG Jun[Δ], WANG Jiajing[Δ], LI Deyun, HOU Jing, LI Jiankuan, BAI Yun'e, GAO Jianping[*]

School of Pharmaceutical Science, Shanxi Medical University, Jinzhong 030600, China

Available online 20 Mar., 2024

[ABSTRACT] Inulin-type fructan CP-A, a predominant polysaccharide in *Codonopsis pilosula*, demonstrates regulatory effects on immune activity and anti-inflammation. The efficacy of CP-A in treating ulcerative colitis (UC) is, however, not well-established. This study employed an *in vitro* lipopolysaccharide (LPS)-induced colonic epithelial cell model (NCM460) and an *in vivo* dextran sulfate sodium (DSS)-induced colitis mouse model to explore CP-A's protective effects against experimental colitis and its underlying mechanisms. We monitored the clinical symptoms in mice using various parameters: body weight, disease activity index (DAI), colon length, spleen weight, and histopathological scores. Additionally, molecular markers were assessed through enzyme-linked immunosorbent assay (ELISA), quantitative real-time polymerase chain reaction (qRT-PCR), immunofluorescence (IF), immunohistochemistry (IHC), and Western blotting assays. Results showed that CP-A significantly reduced reactive oxygen species (ROS), tumor necrosis factor-alpha (TNF-α), and interleukins (IL-6, IL-1β, IL-18) in LPS-induced cells while increasing IL-4 and IL-10 levels and enhancing the expression of Claudin-1, ZO-1, and occludin proteins in NCM460 cells. Correspondingly, *in vivo* findings revealed that CP-A administration markedly improved DAI, reduced colon shortening, and decreased the production of myeloperoxidase (MPO), malondialdehyde (MDA), ROS, IL-1β, IL-18, and NOD-like receptor protein 3 (NLRP3) inflammasome-associated genes/proteins in UC mice. CP-A treatment also elevated glutathione (GSH) and superoxide dismutase (SOD) levels, stimulated autophagy (LC3B, P62, Beclin-1, and ATG5), and reinforced Claudin-1 and ZO-1 expression, thereby aiding in intestinal epithelial barrier repair in colitis mice. Notably, the inhibition of autophagy *via* chloroquine (CQ) diminished CP-A's protective impact against colitis *in vivo*. These findings elucidate that CP-A's therapeutic effect on experimental colitis possibly involves mitigating intestinal inflammation through autophagy-mediated NLRP3 inflammasome inactivation. Consequently, inulin-type fructan CP-A emerges as a promising drug candidate for UC treatment.

[KEY WORDS] Inulin-type fructan CP-A; *Codonopsis pilosula*; Ulcerative colitis; NLRP3 inflammasome; Autophagy
[CLC Number] R965 **[Document code]** A **[Article ID]** 2095-6975(2024)03-0249-16

Introduction

Ulcerative colitis (UC), a subset of inflammatory bowel disease (IBD), is a chronic gastrointestinal disorder marked by inflammation and damage to the intestinal mucosa [1]. The global incidence of UC is escalating, leading the World Health Organization to classify it among modern intractable diseases [2]. UC is characterized by a chronic, relapsing course, alternating between periods of exacerbation and remission [3, 4]. Its primary clinical symptoms include diarrhea, abdominal pain, and the presence of mucus and blood in stools, significantly impairing quality of life [5]. While the exact cause of UC remains elusive, it is internationally acknowledged that its development is associated with impaired immune regulation in the intestinal mucosa, influenced by various environmental factors [6]. Current UC treatments primarily involve anti-inflammatory medications, such as salicylates, glucocorticoids, immunosuppressants, and antibiotics, used as supplementary therapies [7]. However, these treatments often result in a high recurrence rate, adverse side effects, and substantial economic burden [8]. Consequently, the

[Received on] 11-Oct.-2023
[Research funding] This work was supported by the National Natural Science Foundation of China (No. 81904031), National Key Research and Development Program of China (No. 2019YFC1710800), the Natural Science Foundation of Shanxi Province (No. 201901D211325) and the Science Research Start-up Fund for Doctor of Shanxi Medical University (No. XD1802).
[*Corresponding author] E-mail: jpgao123@163.com
[Δ]These authors contributed equally to this work.
These authors have no conflict of interest to declare.

development of complementary and alternative medications is of paramount importance.

NOD-like receptor protein 3 (NLRP3), belonging to the NOD-like receptors (NLRs) family, serves as an essential intracellular immunoreceptor that recognizes a variety of pathogenic microorganisms and endogenous danger signals. Recent studies have identified its crucial role in immune-related diseases [9]. The NLRP3 inflammasome, a multi-molecular complex, typically comprises intracytoplasmic pattern recognition receptors (PRRs), apoptosis-associated speck-like proteins (ASC), and the precursors of aspartate-specific cysteine protease-1 (pro-caspase-1). It plays a vital role in regulating the balance of intestinal commensal bacteria, eliminating harmful bacteria, and synthesizing defensins to maintain intestinal homeostasis [10]. However, in the case of immune abnormalities and impaired intestinal barrier function, which trigger autoimmune responses, the NLRP3 inflammasome becomes overactivated. This overactivation induces the pathological progression of non-infectious intestinal inflammation. ASC recruits pro-caspase-1, leading to self-hydrolysis and activation of caspase-1, which then converts pro-IL-1β and pro-IL-18 into their active forms, IL-1β and IL-18 [11]. Furthermore, caspase-1 plays a pivotal role in a type of inflammatory cell death known as pyroptosis, which results in severe inflammatory responses in the body [12]. Consequently, identifying drug candidates that target the activation of the NLRP3 inflammasome and the subsequent production of IL-1β and IL-18 represents a promising anti-inflammatory strategy for potential UC therapies.

Reactive oxygen species (ROS), a distinct category of oxygenated compounds, are known for their bactericidal properties and role in intestinal defense under normal conditions. Recent research has highlighted that ROS is crucial in the activation of both the NLRP3 inflammasome and autophagy. Mitochondrial dysfunction can stimulate the production of mitochondrial ROS, which in turn activates the NLRP3 inflammasome [13, 14]. Furthermore, activators of NLRP3 can prompt ROS generation, while ROS inhibitors can impede the activation of the NLRP3 inflammasome [15]. ROS also act as effective triggers for cellular autophagy, participating in autophagosome formation and inducing autophagy through multiple signaling pathways [16]. However, cellular autophagy and the inflammasome are not isolated mechanisms; they interact to maintain intracellular dynamic homeostasis under various stress conditions [17]. Cellular autophagy exerts a significant negative regulatory effect on the activation of the NLRP3 inflammasome and regulates ROS and downstream NLRP3 signaling pathways to prevent excessive inflammatory responses. In chronic inflammation, such as UC, excessive ROS produced by neutrophil infiltration can lead to oxidative stress and protein hydrolases, damaging endothelial cells. This damage compromises the intestinal mucosal barrier, facilitating the invasion of intraluminal pathogens, which exacerbate inflammatory cell infiltration and inflammation, culminating in intestinal mucosal necrosis and ulceration [18]. Thus, effectively inhibiting ROS generation is crucial in UC treatment. Additionally, modulating the homeostatic system of autophagy and NLRP3 inflammasome-related pathways to suppress the intestinal inflammatory response may emerge as a key target in UC therapy.

Traditional Chinese Medicine (TCM) and its natural derivatives have a long-standing history in the clinical treatment of various diseases, including UC [19]. Codonopsis Radix, an edible medicinal herb commonly used in TCM for improving gastrointestinal function, originates from the roots of *Codonopsis pilosula*, *C. pilosula* var. *modesta*, and *C. tangshen* [20, 21]. Polysaccharides, believed to be the primary active components, largely contribute to the traditional efficacies of Codonopsis Radix [20]. In recent years, these polysaccharides from Codonopsis Radix have been identified to possess diverse bioactivities, such as immunity modulation, antioxidative, antiviral, anti-inflammatory, and anti-tumor properties [22]. CP-A, an inulin-type fructan, represents one of the most abundant homogeneous polysaccharides extracted from the roots of *C. pilosulae* [23]. Preliminary research by our team has demonstrated that CP-A has a notable protective effect on ethanol-induced acute gastric ulcers in rats [23]. To further explore CP-A's therapeutic potential in gastrointestinal diseases, the current research utilized LPS-induced inflammatory NCM460 cell and dextran sulfate sodium (DSS)-induced colitis mouse models. The aim was to investigate whether CP-A plays a pivotal role in UC treatment by influencing ROS generation, regulating the NLRP3 inflammasome, and promoting cellular autophagy to mitigate inflammatory responses in the intestine. This study lays the groundwork for further refining *Codonopsis* utilization and developing anti-ulcer drugs.

Materials and Methods

Chemicals and reagents

CP-A, an inulin-type fructan with a molecular weight of 3.6 kDa, is a homogeneous polysaccharide isolated using an ultrafiltration method, as described in our previous study [23]. Fig. 1A illustrates the structure of CP-A. DSS was sourced from MP Biomedicals (Irvine, CA, USA, cat. No. 02160110-CF). Chloroquine (CQ) was procured from Sigma-Aldrich (St. Louis, MO, USA, cat. No. C6628-25G). Sulfasalazine (SASP) was obtained from Xinyitianping Pharmaceutical Co., Ltd. (Shanghai, China). All other chemicals, reagents, and solvents used were of analytical grade.

Cells culture and CCK-8 assay

Human NCM460 colonocytes were acquired from Shanghai PiTuo Biotechnology Co., Ltd. and cultured in RPMI-1640 medium (Gibco, NY, USA, cat. No. 31870-074) supplemented with 10% fetal bovine serum (FBS, AusGeneX, Australia, Cat. No. 10100147) and 1% streptomycin/penicillin (Gibco, NY, USA, cat. No. 15240-062). The culture conditions were maintained at 37 °C in an atmosphere of 95% air and 5% CO_2. The Cell Counting Kit-8 (CCK-8) assay was employed to assess cell viability. NCM460 cells

(5×10^4 cells/mL) were seeded into 96-well plates and treated with various concentrations of CP-A (0−500 μg·mL^{-1}) for 24 h to evaluate cell viability. To examine CP-A's protective role in the *in vitro* model, cells were pre-treated with selected low, medium, and high concentrations of CP-A, as well as indomethacin (Indo, as the positive control drug), for 2 h, followed by incubation with lipopolysaccharide (LPS) (100 ng·mL^{-1}) for 24 h [24]. Subsequently, 10 μL of CCK-8 reagent was added to each well and incubated at 37 °C for 2 h. The optical density (*OD*) at 450 nm was measured using an automatic microplate reader (Allsheng, AMR-100, Hangzhou, China).

ROS assay

NCM460 cells underwent treatment with varying concentrations of CP-A for 2 hours, followed by incubation with or without LPS for 24 h. The total intracellular ROS levels were quantified using dichlorodihydrofluorescein diacetate (DCFH-DA) staining, in line with the manufacturer's instructions (Elabscience, Wuhan, China, cat. No. E-BC-K138-F). The procedure involved discarding the cell culture medium

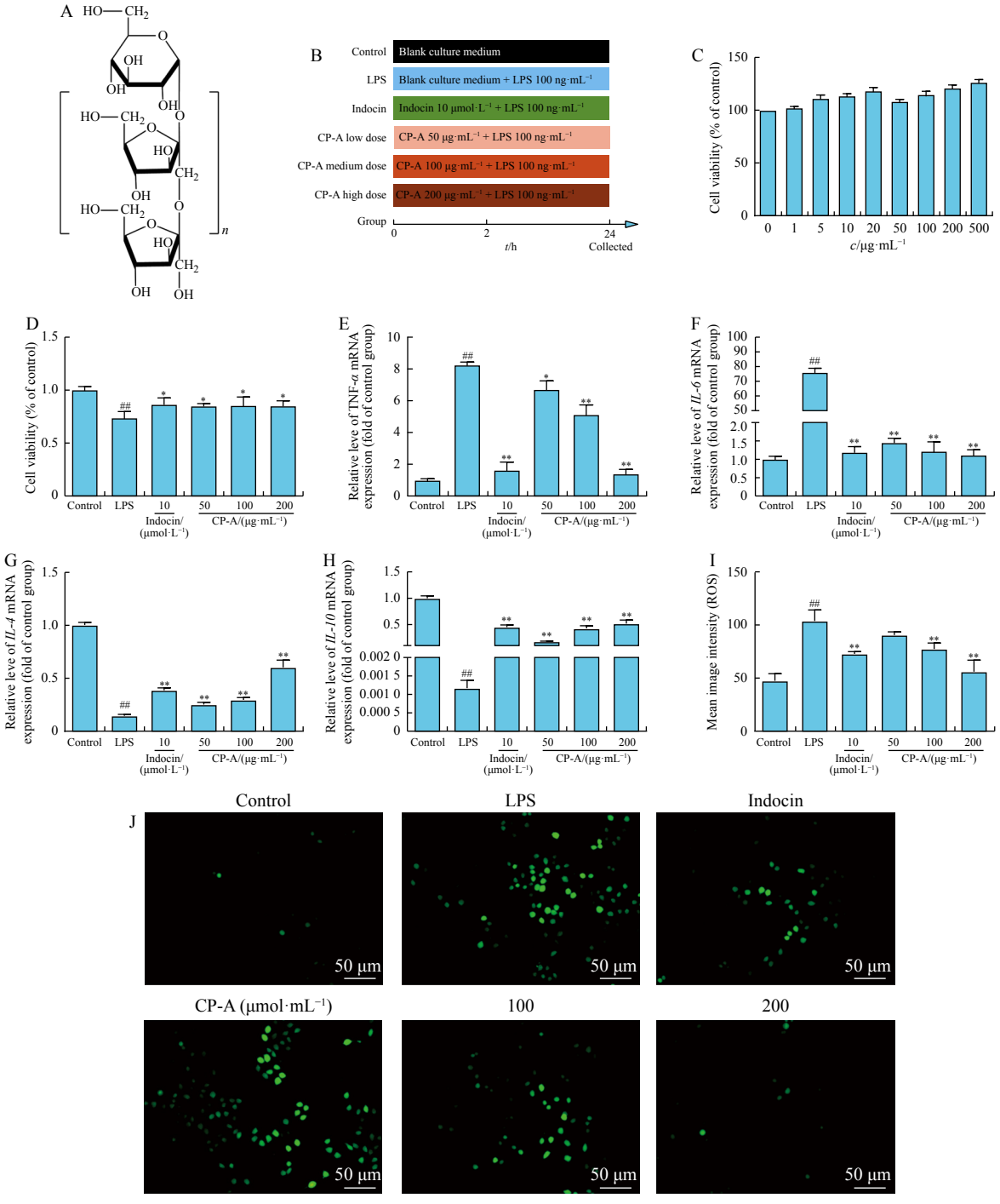

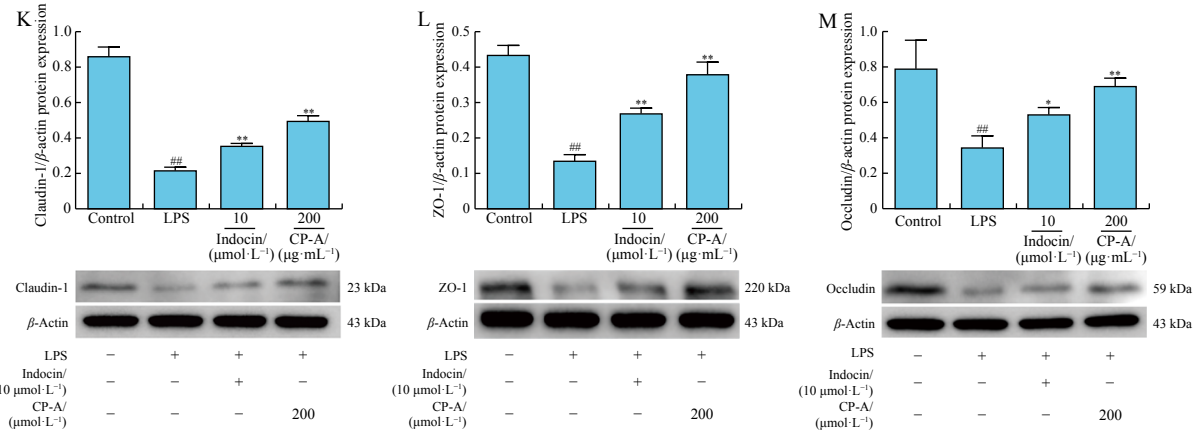

Fig. 1 CP-A attenuated the inflammatory response in LPS-induced inflammation in NCM460 cells. (A) The chemical structure of CP-A. (B) Experimental design and study grouping. (C) Cell viability was measured by CCK-8. (D) The protective effect of CP-A in LPS-induced NCM460 cells was detected by CCK-8 assay. The mRNA expression of inflammatory factors was determined by qRT-PCR. (E) *TNF-α*. (F) *IL-6*. (G) *IL-4*. (H) *IL-10*. (I&J) DCFH-DA staining was performed to detect intracellular ROS. The values are presented as mean ± SD (n = 6). $^{\#}P < 0.05$, $^{\#\#}P < 0.01$ *vs* control; $^{*}P < 0.05$, $^{**}P < 0.01$ *vs* LPS group. The effects of CP-A on the epithelial barrier function in NCM460 cells were examined by Western blotting. (K) Claudin-1. (L) ZO-1. (M) Occludin. The values of Western blotting are presented as mean ± SD (n = 3). $^{\#}P < 0.05$, $^{\#\#}P < 0.01$ *vs* control; $^{*}P < 0.05$, $^{**}P < 0.01$ *vs* LPS group.

and adding DCFH-DA at a final concentration of 10 μmol·L^{-1} to each well, followed by a 1-hour incubation. Subsequently, the cells were washed with PBS to remove excess DCFH-DA. Observations were made using an inverted fluorescence microscope (Leica, Germany, magnification ×20), and the results were quantified using ImageJ software version 1.46 (National Institutes of Health, Bethesda, MD, USA).

Experimental animals

Male Balb/c mice, weighing between 22 and 24 grams (approval number: SYXK (Jing) 2017-0005), were obtained from Beijing Sipeifu Biotechnology Co., Ltd.. These animals were housed under specific pathogen-free conditions, with a 12-hour light/dark cycle, at a controlled temperature of 22−24 °C and a humidity range of 40%−55%. They were acclimated to this environment for two weeks, with access to a standard diet and water. The experimental protocol was designed in strict adherence to the ethical standards of the Animal Care and Use Committee of Shanxi Medical University [No. SYXK (Jin) 2019-007] and followed the Guidelines for The Care and Use of Laboratory Animals.

Establishment of DSS-induced colitis models

The animal experiments were structured in two phases. In the first phase, to assess the effect of CP-A on colitis, mice were allocated into six groups (n = 10 each): a control group, a model group, a positive control group (treated with SASP at 200 mg·kg^{-1} *via* intragastric (i.g.) administration), and three CP-A groups (receiving 20, 40, and 80 mg·kg^{-1}, respectively, i.g.). In the second phase, to explore whether CP-A's inhibitory effect on the NLRP3 inflammasome is mediated through autophagy, mice were divided into four groups: a model group, a CQ group (receiving 40 mg·kg^{-1} *via* intraperitoneal (i.p.) injection for autophagy inhibition), a CP-A group (receiving 80 mg·kg^{-1}, i.g.), and a combined CP-A (80 mg·kg^{-1}, i.g.) + CQ (40 mg·kg^{-1}, i.p.) group. Acute ulcerative colitis was induced using a 3% DSS solution for eight consecutive days, as previously described [25]. The chosen CP-A dosages were based on prior literature [23] and preliminary experiments. Mice in the CQ group received an i.p. injection of 40 mg·kg^{-1} CQ every 2 d until the experiment concluded. Treatment groups received their respective drug dosages *via* i.g. administration for 8 d. Clinical manifestations, including body weight, diarrhea, and rectal bleeding, were recorded daily. The Disease Activity Index (DAI) scores were calculated based on existing literature [26]. On the ninth day, mice were anesthetized, and blood samples were collected from the orbital sinus. These samples were then centrifuged at 1000 r·min^{-1} for 10 minutes at 4 °C, and the serum was extracted for analysis. The severity of colon tissue damage was evaluated according to the revised criteria by SU *et al.* [27]. For further analysis, the colorectum was sectioned into three parts for pathological observation, quantitative real-time polymerase chain reaction (qRT-PCR), and Western blotting. Specimens intended for pathological examination were preserved in 4% formaldehyde, while the rest were stored at −80 °C for further analyses.

Histological staining

Colon tissue samples were fixed in 4% paraformaldehyde, embedded in paraffin, and sectioned into 5-μm slices. Hematoxylin and eosin (H&E) staining was conducted, and the histopathological changes in the colon were examined under an Olympus light microscope (Tokyo, Japan). The extent of histopathological alterations was scored based on the criteria outlined in a previous study [28].

Immunohistochemical staining

Immunohistochemical analysis was conducted following the methodology detailed in our prior research [25]. Briefly, paraffin-embedded colon sections were deparaffinized and rehydrated. Following antigen retrieval and the blocking of en-

dogenous peroxidase activity, the slides were incubated overnight at 4 °C with polyclonal antibodies for LC3B (cat. No. ab51520), P62 (cat. No. ab91526), Beclin-1 (cat. No. ab62557), and ATG5 (cat. No. ab228668) (all from Abcam, USA). Subsequently, biotinylated secondary anti-rabbit antibodies were applied and left to incubate at room temperature for 1 h. After 40 min, the sections were stained with DAB (diaminobenzidine) substrate and counterstained with hematoxylin. Images were captured using a Nikon Eclipse Ci scanning microscope (Nikon Instruments, Melville, NY). The integrated optical density (IOD) and the images were analyzed using Image-Pro Plus 6.0 software (Media Cybernetics, Inc., Rockville, MD, USA).

Immunofluorescence staining

Immunofluorescence staining was conducted on paraffin-embedded colon tissues. Following dewaxing and hydration, antigen retrieval was carried out using ethylenediaminetetraacetic acid (EDTA) antigen retrieval buffer (pH 8.0) in a microwave. The sections were then blocked with 3% Bovine Serum Albumin (BSA) for 30 min at room temperature, followed by overnight incubation at 4 °C with primary antibodies against Claudin-1 (cat. No. ab15098), ZO-1 (cat. No. ab96587), and F4/80 (cat. No. ab100790). 4′,6-Diamidino-2-phenylindole (DAPI) staining was subsequently performed. Finally, the sections were visualized and photographed using a Nikon Eclipse C1 fluorescent microscope (Tokyo, Japan).

Analysis of cytokine levels and antioxidant enzyme activities

Colon tissue samples were weighed, homogenized, and centrifuged at 12 000 g for 15 min in a refrigerated centrifuge. The supernatant was then collected for analysis. The levels of myeloperoxidase (MPO), malondialdehyde (MDA), ROS, glutathione (GSH), superoxide dismutase (SOD), interleukin (IL)-1β, and IL-18 were measured following the manufacturer's protocols. Absorbance readings were obtained using a full-wavelength enzyme marker (Meigu, Shanghai, China).

qRT-PCR

Total RNA from NCM460 cells or colon tissues was extracted using the *TransZol Up* reagent (Transgen, Beijing, China, cat. No. ET111-01). The integrity and concentration of the extracted RNA were assessed using an Eppendorf Bioluminometer D30 (Roche, Mannheim, Germany). A one-step gDNA removal and cDNA Synthesis Supermix kit (Transgen, Beijing, China, cat. No. AT311-02) was then used to reversely transcribe 1 μg of total RNA into cDNA, according to the manufacturer's protocol. qRT-PCR analysis was performed using the Tip Green qPCR Supermix (Transgen, Beijing, China, cat. No. AQ141-01) in a Light Cycler^{96} Real-Time PCR System (Roche, Mannheim, Germany). The thermal cycling conditions were set as follows: one cycle at 94 °C for 30 s, followed by 40 cycles at 94 °C for 5 s and 60 °C for 30 s. The specific primer sequences used in the experiments are listed in Supplementary Table S1.

Western blotting assay

Cell and colon tissue samples were lysed using pre-cooled lysis buffer (comprising 10 μL of 100 mmol·L^{-1} PMSF, 10 μL of phosphatase inhibitor, and 1 μL of protease inhibitor per 1 mL of buffer) with an ultrasonic crusher (Scientz, Zhejiang, China) and a tissue grinder (Servicebio, Wuhan, China). Protein concentrations were determined using the BCA protein assay kit (Keygen Biotech, Jiangsu, China, cat. No. KGP902). Proteins were separated by electrophoresis on sodium dodecyl sulfate-polyacrylamide gels of suitable concentration and then transferred to polyvinylidene fluoride membranes. The membranes were incubated with antibodies against Claudin-1 (Cat. No. ab15098), ZO-1 (Cat. No. ab96587), Occludin (Cat. No. ab31721), NLRP3 (Cat. No. ab270449), ASC (Cat. No. ab70627), Interleukin 1 beta (IL-1β) (Cat. No. ab234437), pro-caspase-1 (Cat. No. ab179515), Cleaved caspase-1 p10 (Cat. No. 89332S, Cell Signaling Technology, USA), and *β*-actin (Cat. No. ab179467), all sourced from Abcam, USA. The Bio-Rad ChemiDoc XRS imaging system was used to detect the intensity of the protein bands, which were analyzed using Image Lab Software 6.0 (Bio-Rad Laboratories).

Statistical analysis

The data from three independent experiments are presented as Mean ± Standard Deviation (SD). Statistical analyses were conducted using Statistical Package for the Social Sciences (SPSS) software (version 26.0, IBM, New York, USA) and GraphPad Prism 8.0 (San Diego, USA). The Student's *t*-test or one-way Analysis of Variance (ANOVA) was applied to identify significant differences, followed by Lysergic Acid Diethylamide (LSD) or Dunnett's T3 post hoc test. A *P*-value of < 0.05 was considered statistically significant.

Results

Protective effects of CP-A on NCM460 colonocytes against LPS-induced injury

The experimental design for the cell studies is depicted in Fig. 1B. The CCK-8 assay was utilized to evaluate CP-A's protective impact on NCM460 cells against LPS-induced damage. As illustrated in Fig. 1C, CP-A concentrations ranging from 1 to 500 μg·mL^{-1} were found to be non-toxic to NCM460 cells. Based on preliminary experiments, doses of 50, 100, and 200 μg·mL^{-1} were selected as low, medium, and high doses, respectively, for further testing. Fig. 1D demonstrates that following LPS treatment, the survival rate of NCM460 cells significantly decreased in comparison to the control group ($P < 0.01$). However, treatment with CP-A at all tested doses significantly enhanced cell survival in a dose-dependent manner ($P < 0.05$).

Suppression of CP-A on release of inflammatory factors in LPS-stimulated NCM460 cells

The mRNA levels of *TNF-α*, *IL-6*, *IL-4*, and *IL-10* in NCM460 cells were quantified using qRT-PCR analysis. Figs. 1E−1H indicate that LPS notably increased the mRNA expression levels of pro-inflammatory factors (TNF-α and IL-6) and decreased the expression of anti-inflammatory factors

(IL-4 and IL-10) in NCM460 cells, compared with the control group ($P < 0.01$). Conversely, pre-treatment with CP-A significantly reduced the expression of pro-inflammatory factors and increased the expression of anti-inflammatory factors in a concentration-dependent manner ($P < 0.01$). Notably, the 200 μg·mL^{-1} dose of CP-A showed the most pronounced inhibitory effect.

Improvement of CP-A on the clinical symptoms in DSS-induced colitis in mice

Oral administration of DSS is known to induce a colitis model in mice that closely mimics the clinical symptoms of human UC, including weight loss, diarrhea, and rectal bleeding [29]. To evaluate CP-A's beneficial effects against UC, a mouse model was developed using a continuous 3% DSS solution feed for 8 d. The experimental protocol is illustrated in Fig. 2A. Relative to the control group, mice in the DSS group exhibited continuous weight loss (Fig. 2B), significantly elevated Disease Activity Index (DAI) scores (Fig. 2C), and splenomegaly (Fig. 2D). Following treatment with CP-A and SASP, the mice's body weight began to recover from day 5. Additionally, both DAI scores and spleen indexes significantly decreased ($P < 0.01$).

Colon length and macroscopic appearance are critical indicators of the severity of colorectal inflammation [29]. As depicted in Figs. 2E−2G, control mice had healthy colons without ulcers. In contrast, the DSS group exhibited shortened colons with visible signs of edema, congestion, intestinal wall thickening, mucosal erosion, ulceration, and adhesion to adjacent tissues. Treatment with CP-A and SASP notably mitigated colon shortening ($P < 0.01$) and improved the aforementioned clinical symptoms. Measurements of colon length aligned with macroscopic scores. Histological analysis further demonstrated that DSS administration led to colonic inflammation, characterized by epithelial crypt loss, mucosal barrier disruption, and inflammatory cell infiltration, resulting in higher histological scores (Figs. 2H & 2I). Conversely, treatment with CP-A and SASP significantly reduced severe histologic inflammation, thereby markedly lowering microscopic scores. Additionally, CP-A notably reduced the distribution of F4/80+ macrophages in the colonic lamina propria (Fig. 2J).

Elimination of CP-A on oxidative stress in the colorectum of DSS-induced mice

Figs. 3A−3E demonstrate that DSS administration significantly elevated levels of myeloperoxidase (MPO), malondialdehyde (MDA), and ROS while notably reducing superoxide dismutase (SOD) and glutathione (GSH) levels compared to the control group ($P < 0.01$). However, treatment with SASP and CP-A effectively mitigated oxidative stress by decreasing MPO, MDA, and ROS levels and enhancing SOD and GSH contents in colon tissues relative to the DSS group ($P < 0.01$). Corresponding with *in vivo* results, cellular experiments also indicated that CP-A significantly reduced the elevation of ROS content due to LPS stimulation (Figs 1I & 1J).

Enhancement of CP-A on the epithelial barrier function in DSS-induced colitis in mice

The expression of Claudin-1, ZO-1, and Occludin is essential for maintaining intestinal mucosal barrier function [30]. Initially, Western blotting analysis was used to assess the protein expression of Claudin-1, ZO-1, and Occludin in NCM460 cells (Figs. 1K−1M). Following LPS stimulation of intestinal epithelial cells (IECs), the protein levels of Claudin-1, ZO-1, and Occludin were observed to decrease significantly ($P < 0.01$). Conversely, CP-A pre-treatment significantly upregulated these protein levels ($P < 0.01$). In line with the *in vitro* results, immunohistochemical staining revealed that DSS exposure significantly reduced Claudin-1 and ZO-1 immunoreactivity in colon tissues. However, more pronounced immunoreactivity was observed in the SASP and CP-A groups compared to the DSS group (Figs. 4A & 4B). These results strongly suggest that CP-A's effect on DSS-induced UC in mice is associated with the regulation of colonic mucosal barrier function.

Inhibition of CP-A on the activation of NLRP3 inflammasome in DSS-induced colitis in mice

The NLRP3 inflammasome, comprising the core protein complex (NLRP3-ASC-pro-caspase-1 assembly), plays a critical role in the inflammatory response associated with DSS-induced colitis in mice [31]. To explore whether CP-A's protective effect is linked to inhibiting NLRP3 inflammasome activation, the expression levels of related genes and proteins were measured using qRT-PCR and Western blotting assays. Figs. 5A−5F demonstrate that the protein expressions of NLRP3 and ASC were significantly elevated following DSS exposure, whereas CP-A treatment notably suppressed these protein expressions. Prior studies indicate that NLRP3 inflammasome activation can prompt the hydrolysis of pro-caspase-1 to generate caspase-1 while facilitating the secretion or expression of IL-1β and IL-18 through the cleavage of their proenzyme forms [32]. Crucially, our study revealed that pro-caspase-1 protein levels were significantly increased, but the expression of caspase-1 p10 was inhibited in both CP-A and SASP treatment groups. Moreover, a combination of qRT-PCR, enzyme-linked immunosorbent assay (ELISA), and Western blotting results showed that DSS stimulation caused an upregulation in protein (Figs. 5G & 5H) and gene (Figs. 5I & 5J) expressions of IL-1β and IL-18 ($P < 0.01$−0.05). In contrast, CP-A significantly reduced the protein and gene expressions of IL-1β and IL-18 ($P < 0.01$−0.05), highlighting its role in mitigating the inflammatory response in DSS-induced colitis.

Effects of CP-A on inactivation of NLRP3 inflammasome by promoting autophagy

LC3B, P62, Beclin-1, and ATG5 are recognized biomarkers of autophagy [33]. Immunohistochemical analysis revealed a significant reduction in LC3B and Beclin-1 (Figs. 6B & 6C) and a marked increase in P62 (Fig. 6D) following DSS stimulation. In contrast, CP-A treatment notably pro-

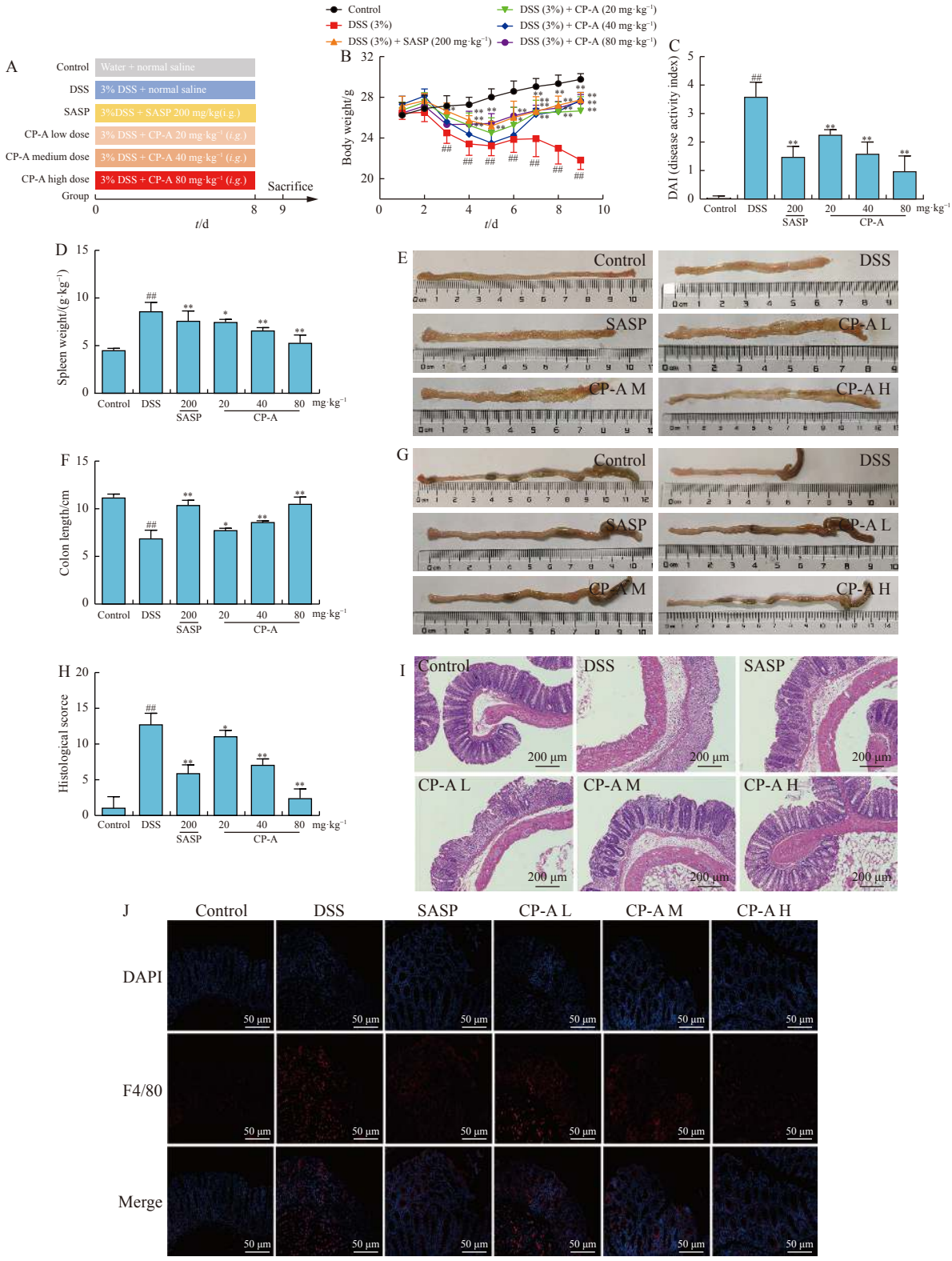

Fig. 2 CP-A ameliorated DSS-induced acute colitis in mice. (A) Experimental design and study grouping. (B) Body weight Changes. (C) Disease activity indexes. (D) Splenic indexes. (E) Colon appearance in longitudinal section. (F) Colon length. (G) Visual appearance of colon tissue. (H) Histopathological scores. (I) H&E stained sections (magnification 200 ×). (J) Immunofluorescence assay for detecting F4/80+ macrophage infiltration in colon tissue (magnification 200 ×). CP-A L, low dose of CP-A (20 mg·kg^{-1}, i.g); CP-A M, medium dose of CP-A (40 mg·kg^{-1}, i.g); CP-A H high dose of CP-A (80 mg·kg^{-1}, i.g). The values are presented as mean ± SD of 6 mice in each group. $^{\#}P < 0.05$, $^{\#\#}P < 0.01$ *vs* control; $^{*}P < 0.05$, $^{**}P < 0.01$ *vs* DSS group.

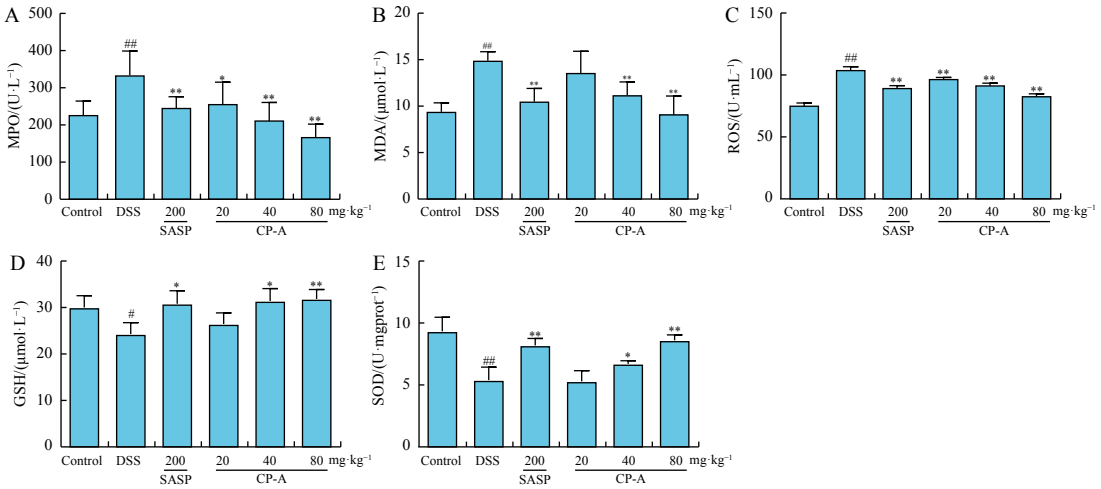

Fig. 3 CP-A eliminated the oxidative stress in DSS-stimulated colitis in mice. (A) MPO. (B) MDA. (C) ROS. (D) GSH. (E) SOD. The values are presented as the mean ± SD (n = 6). $^{\#}P < 0.05$, $^{\#\#}P < 0.01$ *vs* control; $^{*}P < 0.05$, $^{**}P < 0.01$ *vs* DSS group.

moted autophagy (P < 0.01−0.05). The qRT-PCR results, depicted in Figs. 6F−6H, corroborated these immunohistochemical findings. ATG5 plays a crucial role in initiating the autophagic process and modulating the activation of the NLRP3 inflammasome [34]. The immunohistochemical staining and qRT-PCR analysis results showed that CP-A significantly enhanced both the gene and protein expression of ATG5 in the colons of mice with DSS-induced colitis (Figs. 6E & 6I, P < 0.05). These findings substantiate the pivotal role of ATG5-mediated autophagy in the CP-A-induced inactivation of the NLRP3 inflammasome, contributing to the alleviation of DSS-induced colitis. This suggests that CP-A's therapeutic action

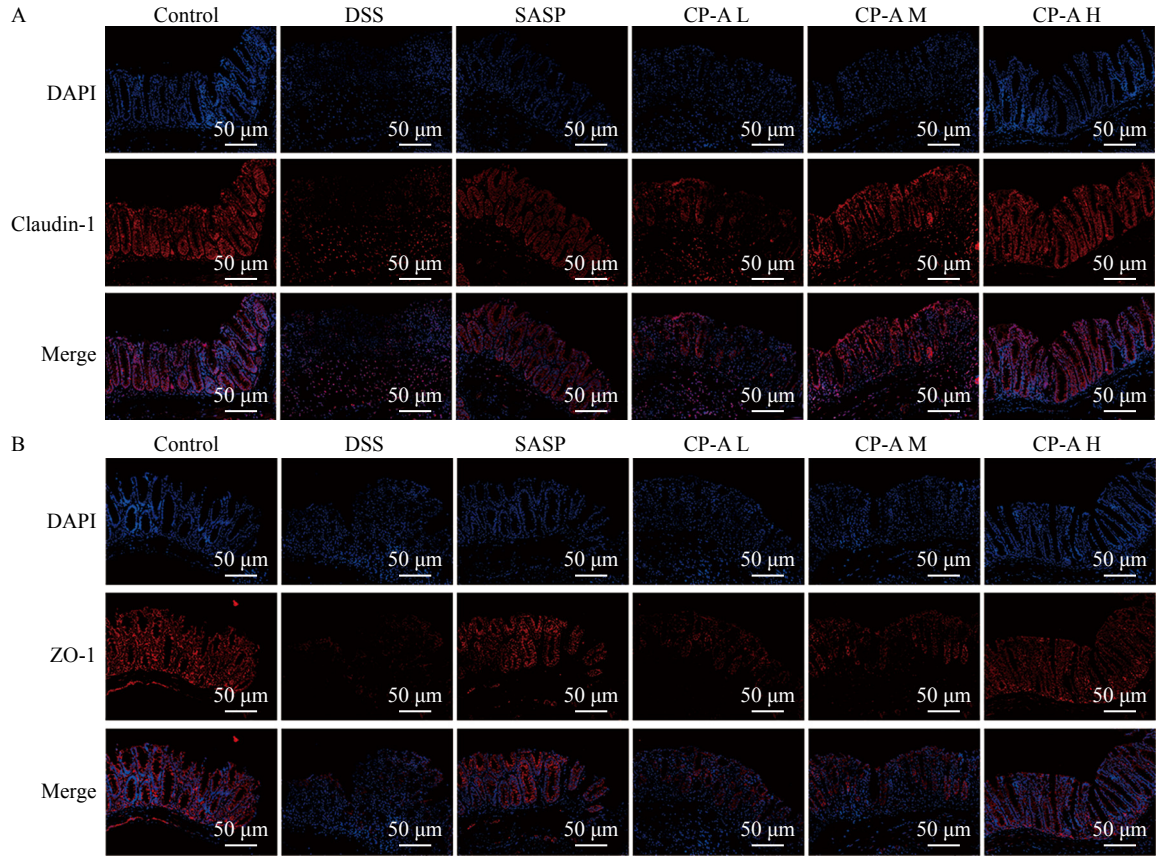

Fig. 4 CP-A enhanced the epithelial barrier function in DSS-induced colitis in mice. (A) Colon tissue stained with Claudin-1 (red) and nuclei-stained with DAPI (blue). (B) Colon tissue stained with ZO-1 (red) and nuclei-stained with DAPI (blue). Fluorescence images were captured using a fluorescence microscope (magnification 200 ×). CP-A L, low dose of CP-A (20 mg·kg^{-1}, i.g); CP-A M, medium dose of CP-A (40 mg·kg^{-1}, i.g); CP-A H high dose of CP-A (80 mg·kg^{-1}, i.g).

in UC may involve the modulation of autophagy pathways, highlighting its potential as a treatment option.

Attenuating effects of autophagy inhibition on the protective role of CP-A in DSS-induced colitis in mice

To explore the interplay between autophagy and CP-A's protective effect, we established a UC mouse model treated with the autophagy inhibitor CQ. The experimental design and group allocations are illustrated in Fig. 7A. The study revealed that the autophagy-promoting effect of CP-A (80 mg·kg^{-1}, orally) was significantly diminished in the UC mouse model when autophagy was inhibited. Figs. 7B−7I show that the inhibition of autophagy notably compromised the beneficial effects of CP-A. This was evidenced by increased weight loss, higher disease activity indexes, reduced splenic indexes, shortened colon length, and exacerbated colonic inflammation. It was also observed that in CP-A-treated colitis mice, CQ pre-treatment mitigated the reduction in pro-inflammatory cytokines and the restoration of colonic epithelial barrier function (Figs. 7J−7L). Immunohistochemistry (IHC) results (Figs. 8A−8E) indicated that, compared to the CP-A group, the expression of autophagy-related markers (LC3B, Beclin-1, and ATG5) decreased, and P62 expression increased in the CQ + CP-A group. Furthermore, Western blotting results demonstrated that the activation of the NLRP3 inflammasome, which was reduced by CP-A treatment, was less pronounced following CQ pre-treatment (Figs. 8F−8J). Collectively, these findings suggest that the protective effect of CP-A in the UC mouse model is atten-

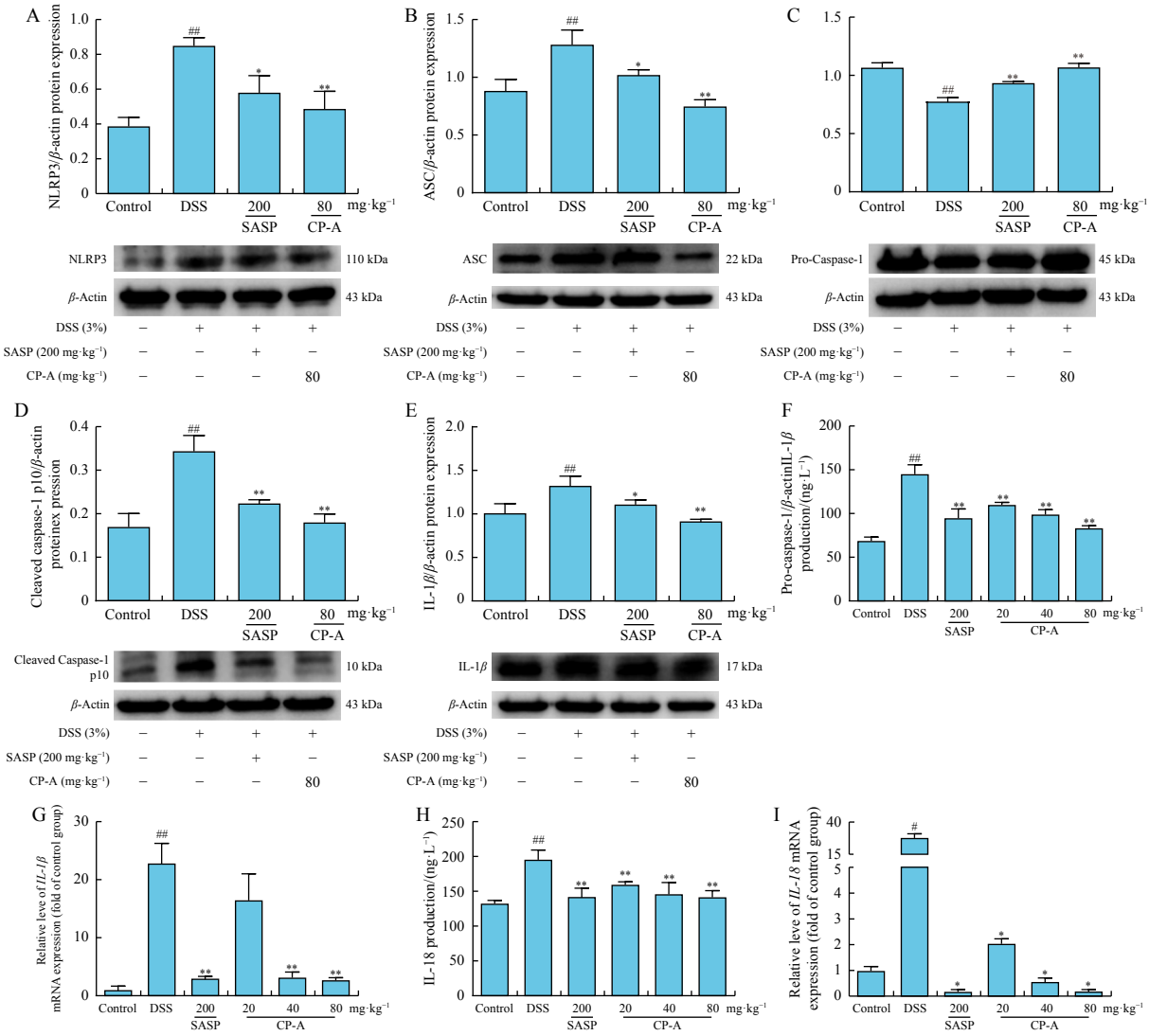

Fig. 5 CP-A abrogated the NLRP3 inflammasome in DSS-induced colitis in mice. The key protein expressions of NLRP3 inflammasome were detected by Western blotting. (A) NLRP3. (B) ASC. (C) Pro-caspase-1. (D) Cleaved caspase-1 p10. (E) IL-1β. The values of Western blotting are presented as mean ± SD (n = 3). $^{\#}P < 0.05$, $^{\#\#}P < 0.01$ *vs* control; $^{*}P < 0.05$, $^{**}P < 0.01$ *vs* DSS group. The content of (F) IL-1β and (H) IL-18 in colitis mice were measured by ELISA kits. The mRNA levels of (G) *IL-1β* and (I) *IL-18* in colitis mice were observed by qRT-PCR. The values are presented as the mean ± SD (n = 6). $^{\#}P < 0.05$, $^{\#\#}P < 0.01$ *vs* control; $^{*}P < 0.05$, $^{**}P < 0.01$ *vs* DSS group.

uated when autophagy is inhibited, underscoring the importance of autophagy in mediating CP-A's therapeutic action in UC.

Discussion

UC, or ulcerative colitis, is a chronic, recurrent idiopathic inflammatory disorder of the gastrointestinal tract. Despite extensive research, its exact etiology remains elusive, and therapeutic options are limited [35]. Consequently, the discovery of new effective treatments or adjunctive therapies is critical. In this study, CP-A was validated for the first time as a regulator of intestinal mucosal inflammation, epithelial barrier function, and autophagy in UC models.

Our research delved into the anti-colitis effects of CP-A through both *in vitro* and *in vivo* experiments. IECs are pivotal in regulating gut immune homeostasis, and impaired epithelial responses have been implicated in the pathogenesis of inflammatory bowel diseases [36]. LPS, a component of the outer cell wall of Gram-negative bacteria, is known to induce inflammatory reactions, apoptosis, and autophagy [37, 38]. Therefore, we initially established an *in vitro* UC model using human normal colonic epithelial cells (NCM460) challenged with LPS. Our findings distinctly highlight CP-A's cytoprotective effect on LPS-induced NCM460 cells, characterized by a decrease in pro-inflammatory cytokines (TNF-α and IL-6) and an increase in anti-inflammatory factors (IL-

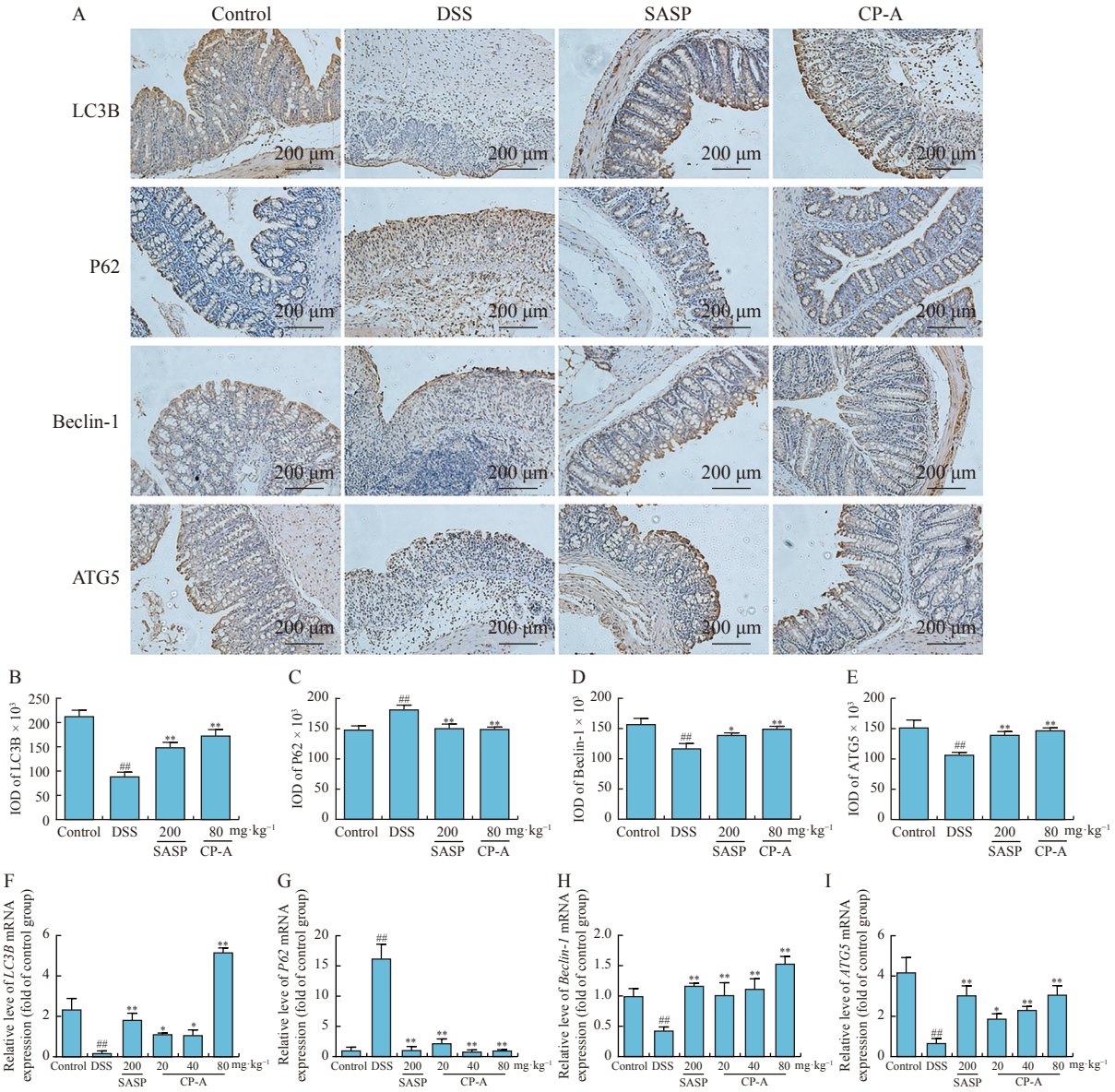

Fig. 6 CP-A prompted autophagy in DSS-induced colitis in mice. The biomarkers of autophagy were estimated by immunohistochemical analysis. (A) Representative immunohistochemical staining (original magnification 200 ×). (B) IOD of LC3B. (C) IOD of P62. (D) IOD of Beclin-1. (E) IOD of ATG5. The mRNA levels of (F) *LC3B*, (G) *P62*, (H) *Beclin-1*, and (I) *ATG5* were detected by qRT-PCR. The values are are presented as mean ± SD (n = 6). $^{\#\#}P < 0.01$ *vs* control; $^{*}P < 0.05$, $^{**}P < 0.01$ *vs* DSS group.

4 and IL-10). Oral administration of DSS disrupts the integrity of the colonic epithelial barrier, allowing intestinal bacteria to enter and stimulate underlying tissues, leading to inflammatory cell infiltration. This process is commonly used to induce inflammation in experimental models [39]. In our study, CP-A significantly mitigated weight loss, elevated DAI, and reduced colon length in colitis mice. Histopathological analysis further revealed that CP-A pretreatment markedly decreased neutrophil infiltration in the colon. MPO, primarily found in neutrophils, serves as a marker of neutrophil infiltration and acute inflammation [40]. Additionally, the overproduction of MPO activity-mediated nitric oxide (NO) is considered an inflammatory biomarker and may directly contribute to tissue damage [41]. Our research demonstrated that CP-A effectively attenuated the abnormal elevation of MPO in a dose-dependent manner, indicating its potent anti-

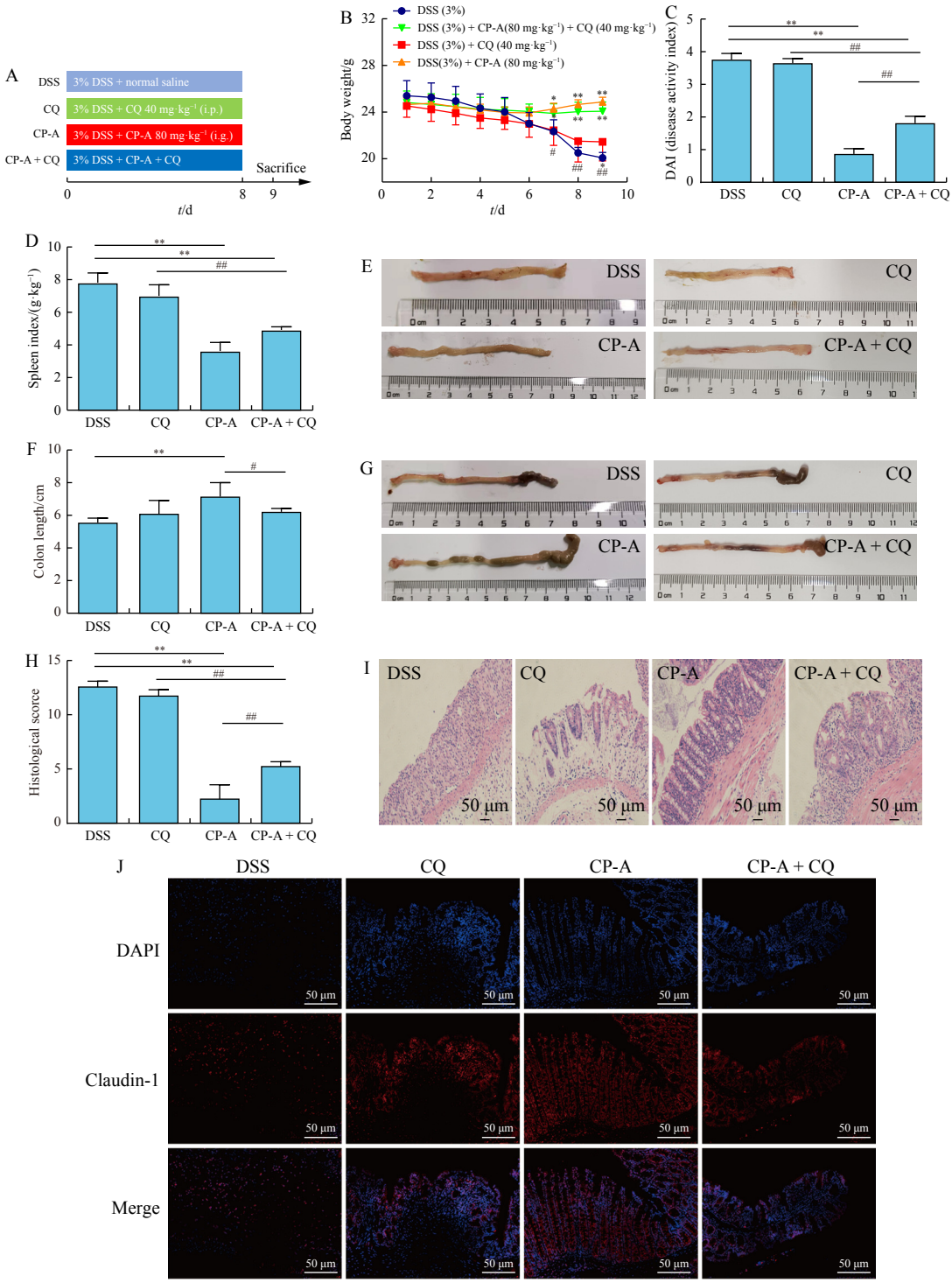

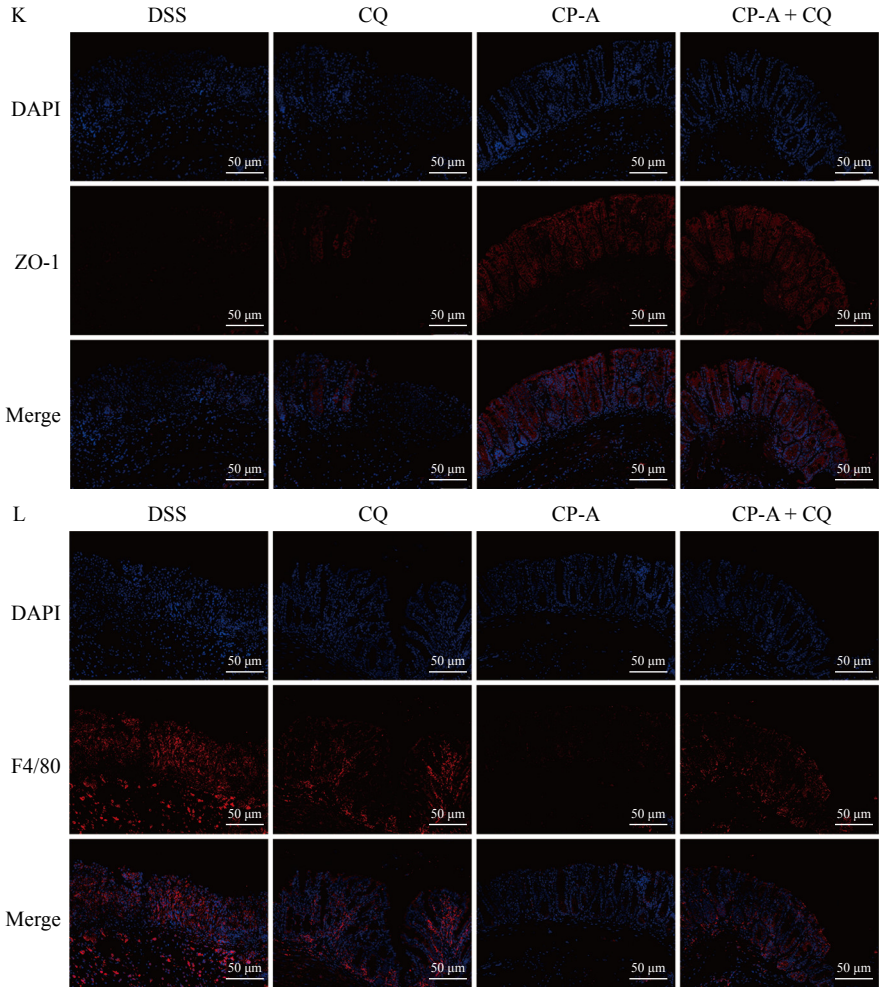

Fig. 7 Attenuating effects of autophagy inhibition on the protective role of CP-A in DSS-induced colitis in mice. (A) Experimental design and study grouping. (B) Body weight changes. (C) Disease activity indexes. (D) Splenic indexes. (E) Colon appearance in longitudinal section. (F) Colon length. (G) Visual appearance of colon tissue. (H) Histopathological scores. (I) H&E stained sections (magnification 200×). Immunofluorescence assay for detecting infiltration of (J) Claudin-1, (K) ZO-1, and (L) F4/80 + macrophages in colon tissue, images taken at a magnification of 200×. The values are presented as mean ± SD of 6 mice in each group. $^{*}P < 0.05$, $^{**}P < 0.01$ *vs* DSS; $^{\#}P < 0.05$, $^{\#\#}P < 0.01$ *vs* CPA + CQ group.

inflammatory effects on DSS-induced acute colitis. This underlines the potential of CP-A as a novel therapeutic agent in managing UC, offering a promising avenue for future drug development in this field.

IECs are crucial as the primary defense in the intestinal mucosal barrier [42]. Dysfunctions in the epithelial barrier can lead to dysbiosis of the intestinal microbiota and immune system abnormalities, triggering inflammation [43, 44]. While there is ongoing debate about whether the impairment of epithelial barrier function is a consequence of chronic inflammation or a causative factor in UC, it is well-established that epithelial barrier dysfunction is a common characteristic in all UC patients [45]. Claudin-1, ZO-1, and Occludin are key tight junction proteins instrumental in maintaining the integrity of the intestinal mucosal barrier [46]. The findings of this study revealed that the expression levels of Claudin-1 and ZO-1 were significantly downregulated in both IECs and mouse intestinal tissues in the context of inflammation. Conversely, CP-A pretreatment notably upregulated the expression of Claudin-1 and ZO-1 and reduced the histological score of colonic mucosal injury. These results suggest that CP-A may alleviate inflammation by restoring intestinal epithelial barrier function. Moreover, there exists a close connection between autophagy and the intestinal epithelial tight junction barrier, with evidence suggesting that autophagy can enhance intestinal barrier function [47]. However, the precise relationship between autophagy and intestinal barrier integrity remains to be fully elucidated, warranting further research. Understanding this relationship could provide deeper insights into the pathophysiology of UC and highlight novel therapeutic targets, potentially including the modulation of autophagy as a strategy to restore or strengthen the intestinal barrier in UC patients.

Autophagy, a lysosome-mediated programmed cell degradation pathway, plays a pivotal role in maintaining cellular homeostasis [48]. Both excessive and insufficient auto-

phagy can contribute to the development of organ-specific diseases. In the context of UC, there is a notable association with defective autophagy [49]. ROS, potent activators of autophagy, can participate in autophagosome formation and induce autophagy through various signaling pathways [50]. Cellular autophagy negatively regulates the activation of the NLRP3 inflammasome and is involved in controlling ROS and downstream NLRP3 signaling pathways, thus preventing excessive inflammatory responses [51]. Additionally, ROS-mediated oxidative stress can activate the autophagy pathway to eliminate damaged macromolecules, thereby preserving cellular homeostasis [52]. Our study revealed that CP-A significantly inhibited the excessive generation of ROS in human colonic epithelial cells and mouse colon tissue under DSS-induced stress, thereby reducing apoptosis in colonic cells. CP-A was also shown to elevate levels of GSH and SOD, helping to regulate or eliminate excess ROS and thus maintain cellular homeostasis. Autophagy is characterized by increased levels of autophagy-related proteins (e.g., LC3-I to LC3-II conversion, Beclin-1, ATG5) and decreased levels of p62 [53]. Autophagy acts as a pro-survival response under various stresses by recycling metabolic substrates to maintain energy homeostasis [54]. Consistently, our data indicated that CP-A promoted autophagy, aligning with previous findings that its therapeutic effect on colitis may relate to autophagy activation. IL-1β and IL-18, produced by the NLRP3 inflammasome, are recognized as critical pathogenic factors in UC progression. Clinical studies have correlated elevated IL-1β levels with the severity of IBD, and preclinical studies suggest IL-18's contribution to colitis pathogenesis [55-58]. Our study observed significant increases in IL-1β and IL-18 in the colonic mucosae of mice with DSS-induced colitis, which were reduced by CP-A treatment. Furthermore, CP-A decreased the levels of NLRP3, ASC, and caspase-1 p10. Emerging evidence indicates that inhibiting the NLRP3 inflammasome can trigger autophagy activation [59]. Our study examined whether CP-A regulates NLRP3 inflammasome activation through autophagy. We found that CP-A promoted autophagy in DSS-induced colitis, while the autophagy inhibitor CQ blocked CP-A's protective effects, suggesting autophagy's involvement in CP-A-mediated UC improvement. Conversely, inducing autophagy has been reported to suppress NLRP3 inflammasome activation in rats [60], and autophagy inhibition is known to activate the NLRP3 inflammasome in macrophages [61]. Thus, the exact relationship between autophagy and the NLRP3 inflammasome remains a

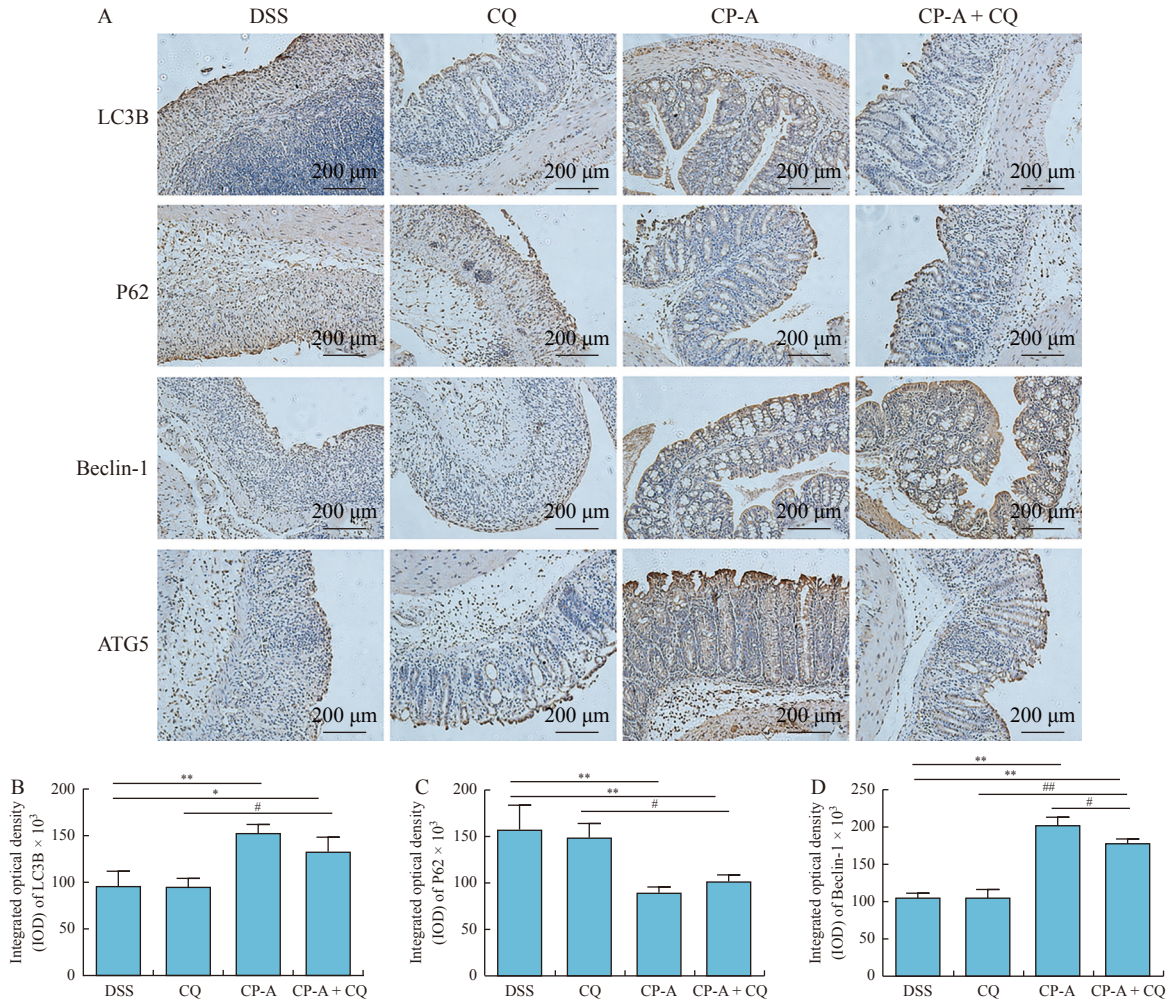

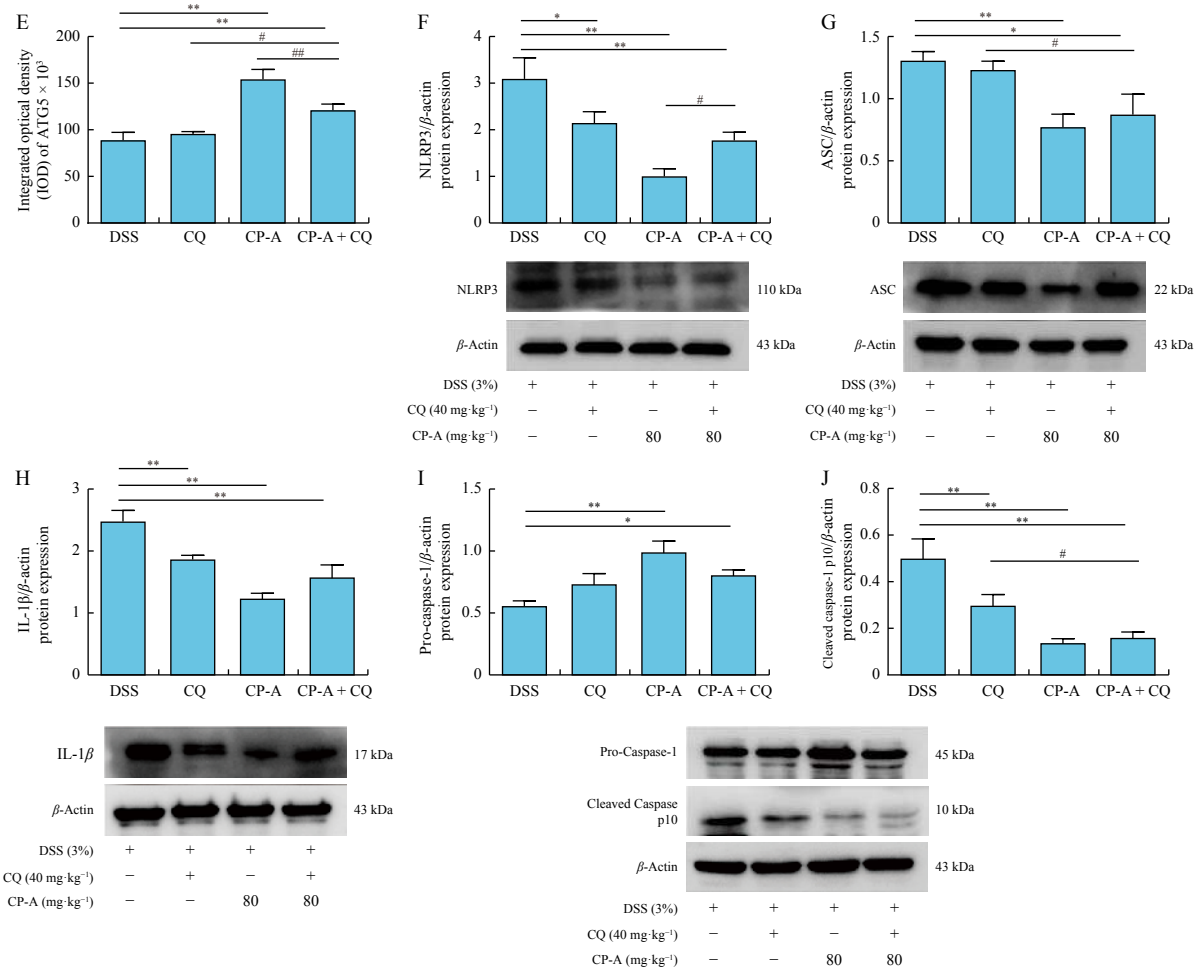

Fig. 8 Attenuating effects of autophagy inhibition on the protective role of CP-A in DSS-induced colitis in mice. The biomarkers of autophagy were estimated by immunohistochemical analysis. (A) Representative immunohistochemical staining (original magnification 200×). (B) *IOD* of LC3B. (C) *IOD* of P62. (D) *IOD* of Beclin-1. (E) *IOD* of ATG5. The key protein expressions of NLRP3 inflammasome were detected by Western blotting. (F) NLRP3. (G) ASC. (H) IL-1β. (I) Pro-caspase-1. (J) Cleaved caspase-1 p10. The values of Western blotting are presented as mean ± SD (n = 3). $^{*}P < 0.05$, $^{**}P < 0.01$ *vs* DSS group, $^{\#}P < 0.05$, $^{\#\#}P < 0.01$ *vs* CPA + CQ group.

complex and controversial topic requiring further elucidation. Understanding this relationship could provide crucial insights into novel therapeutic strategies for UC, potentially involving the modulation of autophagy and inflammasome pathways.

In summary, the novel findings from this research demonstrate that CP-A effectively mitigates LPS-induced inflammation in colonic epithelial cells and DSS-stimulated colitis in mice. The underlying mechanism appears to involve, at least in part, the regulation of the balance between autophagy and NLRP3 inflammasome-related pathways, thereby suppressing intestinal inflammation. However, it is important to acknowledge the limitations of this study, which primarily relied on the use of autophagy inhibitors in a mouse model. To further elucidate the anti-colitis effects of CP-A, our future research endeavors will encompass more comprehensive investigations. This includes studies using models of autophagic deficiency, such as mice or cell lines with specific autophagic gene deletions or mutations. These additional studies are crucial for a more in-depth understanding of the mechanisms by which CP-A exerts its anti-inflammatory effects in colitis. By broadening the scope of research to include models with varying levels or patterns of autophagy, we aim to uncover more detailed insights into the intricate interactions between autophagy, the NLRP3 inflammasome, and the inflammatory pathways in UC. These future investigations are expected to contribute significantly to the current understanding of CP-A's mechanism of action in treating colitis. The promising results obtained thus far highlight CP-A's potential as a candidate drug for the treatment of UC. Continued research in this area could pave the way for the development of new therapeutic strategies, potentially improving the management and quality of life for individuals suffering from this chronic and debilitating condition.

Supplementary Materials

The supplementary materials can be requested by sending E-mail to the corresponding author.

References

[1] Su Q, He J, Wang Z, *et al*. Intestinal anti-inflammatory effect of the rhizome extracts of *Menispermum dauricum* DC. on trinitrobenzene sulfonic acid induced ulcerative colitis in mice [J]. *J Ethnopharmacol*, 2016, **193**: 12-20.

[2] Yun J, Xu CT, Pan BR. Epidemiology and gene markers of ulcerative colitis in the Chinese [J]. *World J Gastroenterol*, 2009, **15**(7): 788-803.

[3] Ordas I, Eckmann L, Talamini M, *et al*. Ulcerative colitis [J]. *Lancet*, 2012, **380**(9853): 1606-1619.

[4] Wu N, Du X, Peng Z, *et al*. Silencing of peroxiredoxin 1 expression ameliorates ulcerative colitis in a rat model [J]. *J Int Med Res*, 2021, **49**(3): 0300060520986313.

[5] Chen G, Yang Y, Liu M, *et al*. Banxia Xiexin decoction protects against dextran sulfate sodium-induced chronic ulcerative colitis in mice [J]. *J Ethnopharmacol*, 2015, **166**: 149-156.

[6] Matsuoka K, Kobayashi T, Ueno F, *et al*. Evidence-based clinical practice guidelines for inflammatory bowel disease [J]. *J Gastroenterol*, 2018, **53**: 305-353.

[7] Shaker ME, Ashamallah SA, Houssen ME. Celastrol ameliorates murine colitis *via* modulating oxidative stress, inflammatory cytokines and intestinal homeostasis [J]. *Chem Biol Interact*, 2014, **210**: 26-33.

[8] Wang S, Liu W, Wang J, *et al*. Curculigoside inhibits ferroptosis in ulcerative colitis through the induction of GPX4 [J]. *Life Sci*, 2020, **259**: 118356.

[9] Xu Y, Shen J, Ran Z. Emerging views of mitophagy in immunity and autoimmune diseases [J]. *Autophagy*, 2020, **16**: 3-17.

[10] Zhen Y, Zhang H. NLRP3 inflammasome and inflammatory Bowel disease [J]. *Front Immunol*, 2019, **10**: 276.

[11] Zahid A, Li B, Kombe AJK, *et al*. Pharmacological inhibitors of the NLRP3 inflammasome [J]. *Front Immunol*, 2019, **10**: 2538.

[12] Atianand MK, Rathinam VA, Fitzgerald KA. SnapShot: inflammasomes [J]. *Cell*, 2013, **153**(1): 272-272 e271.

[13] Darisipudi MN, Allam R, Rupanagudi KV, *et al*. Polyene macrolide antifungal drugs trigger interleukin-1beta secretion by activating the NLRP3 inflammasome [J]. *PLoS One*, 2011, **6**: e19588.

[14] Hornung V, Bauernfeind F, Halle A, *et al*. Silica crystals and aluminum salts activate the NALP3 inflammasome through phagosomal destabilization [J]. *Nat Immunol*, 2008, **9**: 847-856.

[15] Lupfer C, Thomas PG, Anand PK, *et al*. Receptor interacting protein kinase 2-mediated mitophagy regulates inflammasome activation during virus infection [J]. *Nat Immunol*, 2013, **14**: 480-488.

[16] Filomeni G, De Zio D, Cecconi F. Oxidative stress and autophagy: the clash between damage and metabolic needs [J]. *Cell Death Differ*, 2015, **22**: 377-388.

[17] Carneiro LA, Travassos LH. The interplay between NLRs and autophagy in immunity and inflammation [J]. *Front Immunol*, 2013, **4**: 361.

[18] Oshitani N, Sawa Y, Hara J, *et al*. Functional and phenotypical activation of leucocytes in inflamed human colonic mucosa [J]. *J Gastroen Hepatol* 1997, **12**(12): 809-814.

[19] Jie F, Xiao S, Qiao Y, *et al*. Kuijieling decoction suppresses NLRP3-mediated pyroptosis to alleviate inflammation and experimental colitis *in vivo* and *in vitro* [J]. *J Ethnopharmacol*, 2021, **264**: 113243.

[20] Li JK, Wang Y, Ji JJ, *et al*. Structural characterization and immunomodulatory activity of a glucan from Radix Codonopsis [J]. *J Funct Foods*, 2021, **83**: 104537

[21] Zou YF, Chen XF, Malterud KE, *et al*. Structural features and complement fixing activity of polysaccharides from *Codonopsis pilosula* Nannf. *var* modesta L.T.Shen roots [J]. *Carbohydr Polym*, 2014, **113**: 420-429.

[22] Guo Y, Shao YY, Zhao YN, *et al*. Pharmacokinetics, distribution and excretion of inulin-type fructan CPA after oral or intravenous administration to mice [J]. *Food Funct*, 2022, **13**: 4130-4141.

[23] Li J, Wang T, Zhu Z, *et al*. Structure features and anti-gastric ulcer effects of inulin-type fructan CP-A from the roots of *Codonopsis pilosula* (Franch.) Nannf [J]. *Molecules*, 2017, **22**(12): 2258

[24] Ding A, Wen X. Dandelion root extract protects NCM460 colonic cells and relieves experimental mouse colitis [J]. *J Nat Med*, 2018, **72**: 857-866.

[25] Zhou J, Wang T, Dou Y, *et al*. Brusatol ameliorates 2,4,6-trinitrobenzenesulfonic acid-induced experimental colitis in rats: involvement of NF-kappaB pathway and NLRP3 inflammasome [J]. *Int Immunopharmacol*, 2018, **64**: 264-274.

[26] Rukshala D, de Silva ED, Ranaweera B, *et al*. Anti-inflammatory effect of leaves of *Vernonia zeylanica* in lipopolysaccharide-stimulated RAW 264.7 macrophages and carrageenan-induced rat paw-edema model [J]. *J Ethnopharmacol*, 2021, **274**: 114030.

[27] Su J, Li C, Yu X, *et al*. Protective effect of pogostone on 2,4,6-trinitrobenzenesulfonic acid-induced experimental colitis *via* inhibition of T Helper cell [J]. *Front Pharmacol*, 2017, **8**: 829.

[28] Liu Q, Zuo R, Wang K, *et al*. Oroxindin inhibits macrophage NLRP3 inflammasome activation in DSS-induced ulcerative colitis in mice *via* suppressing TXNIP-dependent NF-*κ*B pathway [J]. *Acta Pharmacol Sin*, 2020, **41**: 771-781.

[29] Zhou J, Tan L, Xie J, *et al*. Characterization of brusatol self-microemulsifying drug delivery system and its therapeutic effect against dextran sodium sulfate-induced ulcerative colitis in mice [J]. *Drug Deliv*, 2017, **24**: 1667-1679.

[30] Wang J, Zhang C, Guo C, *et al*. Chitosan ameliorates DSS-induced ulcerative colitis mice by enhancing intestinal barrier function and improving microflora [J]. *Int J Mol Sci*, 2019, **20**(22): 5751.

[31] Wang L, Yu Z, Wei C, *et al*. Huaier aqueous extract protects against dextran sulfate sodium-induced experimental colitis in mice by inhibiting NLRP3 inflammasome activation [J]. *Oncotarget*, 2017, **8**: 32937-32945.

[32] Kahlenberg JM, Lundberg KC, Kertesy SB, *et al*. Potentiation of caspase-1 activation by the P2X7 receptor is dependent on TLR signals and requires NF-*κ*B-driven protein synthesis [J]. *J Immunol*, 2005, **175**(11): 7611-7622.

[33] Bai Y, Hou J, Zhang XT, *et al*. *Zanthoxylum bungeanum* seed oil elicits autophagy and apoptosis in human laryngeal tumor cells *via* PI3K/AKT/mTOR signaling pathway [J]. *Anti-cancer Agent Me*, 2021, **21**(18): 2610-2619.

[34] Lv Q, Xing Y, Liu J, *et al*. Lonicerin targets EZH2 to alleviate ulcerative colitis by autophagy-mediated NLRP3 inflammasome inactivation [J]. *Acta Pharm Sin B*, 2021, **11**(9): 2880-2899.

[35] Wu H, Chen QY, Wang WZ, *et al*. Compound sophorae decoction enhances intestinal barrier function of dextran sodium sulfate induced colitis *via* regulating notch signaling pathway in mice [J]. *Biomed Pharmacother*, 2021, **133**: 110937.

[36] Zhang SQ, Ni WK, Xiao MB, *et al*. Actin related protein 3 (ARP3) promotes apoptosis of intestinal epithelial cells in ulcerative colitis [J]. *Pathol Res Pract*, 2019, **215**(2): 235-242.

[37] Hou J, Wang J, Meng J, *et al*. *Zanthoxylum bungeanum* seed oil attenuates LPS-induced BEAS-2B cell activation and inflammation by inhibiting the TLR4/MyD88/NF-*κ*B signaling pathway [J]. *Evid-Based Compl Alt*, 2021, **2021**: 2073296.

[38] Peng Y, Li H, Chen D. Silencing astrocyte elevated gene-1 at-

tenuates lipopolysaccharide-induced inflammation and mucosal barrier injury in NCM460 cells by suppressing the activation of NLRP3 inflammasome [J]. *Cell Biol Int*, 2019, **43**(1): 56-64.
[39] Kim JJ, Shajib MS, Manocha MM, *et al*. Investigating intestinal inflammation in DSS-induced model of IBD [J]. *J Vis Exp*, 2012, (60): 3678.
[40] Jeon YD, Lee JH, Lee YM, *et al*. Puerarin inhibits inflammation and oxidative stress in dextran sulfate sodium-induced colitis mice model [J]. *Biomed Pharmacother*, 2020, **124**: 109847.
[41] Aratani Y. Myeloperoxidase: its role for host defense, inflammation, and neutrophil function [J]. *Arch Biochem Biophys*, 2018, **640**: 47-52.
[42] Peterson LW, Artis D. Intestinal epithelial cells: regulators of barrier function and immune homeostasis [J]. *Nat Rev Immunol*, 2014, **14**: 141-153.
[43] Khan I, Ullah N, Zha L, *et al*. Alteration of gut microbiota in inflammatory Bowel disease (IBD): cause or consequence? IBD treatment targeting the gut microbiome [J]. *Pathogens*, 2019, **8**(3): 126.
[44] Vindigni SM, Zisman TL, Suskind DL, *et al*. The intestinal microbiome, barrier function, and immune system in inflammatory bowel disease: a tripartite pathophysiological circuit with implications for new therapeutic directions [J]. *Therap Adv Gastroenterol*, 2016, **9**: 606-625.
[45] Lechuga S, Ivanov AI. Disruption of the epithelial barrier during intestinal inflammation: quest for new molecules and mechanisms [J]. *Biochim Biophys Acta Mol Cell Res*, 2017, **1864**(7): 1183-1194.
[46] Pan HH, Zhou XX, Ma YY, *et al*. Resveratrol alleviates intestinal mucosal barrier dysfunction in dextran sulfate sodium-induced colitis mice by enhancing autophagy [J]. *World J Gastroenterol*, 2020, **26**(33): 4945-4959.
[47] Nighot PK, Hu CA, Ma TY. Autophagy enhances intestinal epithelial tight junction barrier function by targeting claudin-2 protein degradation [J]. *J Biol Chem*, 2015, **290**(11): 7234-7246.
[48] Zhang H, Lang W, Liu X, *et al*. Procyanidin A1 alleviates DSS-induced ulcerative colitis *via* regulating AMPK/mTOR/p70S6K-mediated autophagy [J]. *J Physiol Biochem*, 2022, **78**: 213-227.
[49] Su S, Wang X, Xi X, *et al*. Phellodendrine promotes autophagy by regulating the AMPK/mTOR pathway and treats ulcerative colitis [J]. *J Cell Mol Med*, 2021, **25**(12): 5707-5720.
[50] Wang Y, Li YB, Yin JJ, *et al*. Autophagy regulates inflammation following oxidative injury in diabetes [J]. *Autophagy*, 2013, **9**: 272-277.
[51] Zhang Y, Liu G, Dull RO, *et al*. Autophagy in pulmonary macrophages mediates lung inflammatory injury *via* NLRP3 inflammasome activation during mechanical ventilation [J]. *Am J Physiol Lung Cell Mol Physiol*, 2014, **307**(2): L173-L185.
[52] Ornatowski W, Lu Q, Yegambaram M, *et al*. Complex interplay between autophagy and oxidative stress in the development of pulmonary disease [J]. *Redox Biol*, 2020, **36**: 101679.
[53] Kim KH, Lee MS. Autophagy-a key player in cellular and body metabolism [J]. *Nat Rev Endocrinol*, 2014, **10**: 322-337.
[54] Parzych KR, Klionsky DJ. An overview of autophagy: morphology, mechanism, and regulation [J]. *Antioxid Redox Signal*, 2014, **20**(3): 460-473.
[55] Yang M, Zhang F, Yang C, *et al*. Oral targeted delivery by nanoparticles enhances efficacy of an Hsp90 inhibitor by reducing systemic exposure in murine models of colitis and colitis-associated cancer [J]. *J Crohns Colitis*, 2020, **14**(1): 130-141.
[56] Zhou Y, Yang M, Yan X, *et al*. Oral nanotherapeutics of andrographolide/carbon monoxide donor for synergistically anti-inflammatory and pro-resolving treatment of ulcerative colitis [J]. *ACS Appl Mater Interfaces*, 2023, **15**(30): 36061-36075.
[57] Yan X, Meng L, Zhang X, *et al*. Reactive oxygen species-responsive nanocarrier ameliorates murine colitis by intervening colonic innate and adaptive immune responses [J]. *Mol Ther*, 2023, **31**(5): 1383-1401.
[58] Ma YA, Zhao JJ, Cheng LL, *et al*. Versatile carbon dots with superoxide dismutase-like nanozyme activity and red fluorescence for inflammatory bowel disease therapeutics [J]. *Carbon*, 2023, **204**: 526-537.
[59] Pavillard LE, Canadas-Lozano D, Alcocer-Gomez E, *et al*. NLRP3-inflammasome inhibition prevents high fat and high sugar diets-induced heart damage through autophagy induction [J]. *Oncotarget*, 2017, **8**: 99740-99756.
[60] Chiu HW, Chen CH, Chang JN, *et al*. Far-infrared promotes burn wound healing by suppressing NLRP3 inflammasome caused by enhanced autophagy [J]. *J Mol Med (Berl)*, 2016, **94**: 809-819.
[61] Dai J, Zhang X, Li L, *et al*. Autophagy inhibition contributes to ROS-producing NLRP3-dependent inflammasome activation and cytokine secretion in high glucose-induced macrophages [J]. *Cell Physiol Biochem*, 2017, **43**(1): 247-256.

Cite this article as: ZHOU Jiangtao, WANG Jun, WANG Jiajing, LI Deyun, HOU Jing, LI Jiankuan, BAI Yun'e, GAO Jianping. An inulin-type fructan CP-A from *Codonopsis pilosula* attenuates experimental colitis in mice by promoting autophagy-mediated inactivation of NLRP3 inflammasome [J]. *Chin J Nat Med*, 2024, **22**(3): 249-264.